Nuclear Inst. and Methods in Physics Research, A 1047 (2023) 167740

Contents lists available at ScienceDirect

Nuclear Inst. and Methods in Physics Research, A

journal homepage: www.elsevier.com/locate/nima

The Cylindrical Drift Chamber of the MEG II experiment

M. Chiappini [a,*], A.M. Baldini [a], H. Benmansour [a,b,c], G. Cavoto [e,f], F. Cei [a,b], G. Chiarello [a], A. Corvaglia [g], F. Cuna [g,h], G. Dal Maso [c,d], M. Francesconi [a,b], L. Galli [a], F. Grancagnolo [g], M. Grassi [a], M. Hildebrandt [c], F. Ignatov [i], M. Meucci [e,f], A. Miccoli [g], W. Molzon [j], D. Nicolò [a,b], A. Oya [k], D. Palo [j], M. Panareo [g], A. Papa [a,b,c], F. Raffaelli [a], F. Renga [e], P. Schwendimann [l], G. Signorelli [a], G.F. Tassielli [m,n], Y. Uchiyama [k], A. Venturini [b], B. Vitali [a,f], C. Voena [e]

[a] INFN Sezione di Pisa, Largo B. Pontecorvo 3, 56127 Pisa, Italy
[b] Dipartimento di Fisica dell'Università, Largo B. Pontecorvo 3, 56127 Pisa, Italy
[c] Paul Scherrer Institut (PSI), 5232 Villigen, Switzerland
[d] Swiss Federal Institute of Technology ETH, 8093 Zürich, Switzerland
[e] INFN Sezione di Roma, Piazzale A. Moro 2, 00185 Rome, Italy
[f] Dipartimento di Fisica dell'Università "Sapienza", Piazzale A. Moro 2, 00185, Rome, Italy
[g] INFN Sezione di Lecce, Via per Arnesano, 73100 Lecce, Italy
[h] Dipartimento di Matematica e Fisica dell'Università del Salento, Via per Arnesano, 73100 Lecce, Italy
[i] Budker Institute of Nuclear Physics of Siberian Branch of Russian Academy of Sciences, 630090, Novosibirsk, Russia
[j] Department of Physics and Astronomy, University of California, Irvine, CA 92697, USA
[k] ICEPP, The University of Tokyo, 7-3-1 Hongo, Bunkyo-ku, Tokyo 113-0033, Japan
[l] Department of Physics, University of Washington, Seattle, WA 98195-1560, USA
[m] INFN Sezione di Bari, Via E. Orabona 4, 70125 Bari, Italy
[n] Dipartimento Interateneo di Fisica "M. Merlin" dell'Università, Via Amendola 173, 70125 Bari, Italy

ARTICLE INFO

Keywords:
Gaseous detector
Drift chamber
Commissioning
Tracking
MEG II
Lepton flavor violation

ABSTRACT

The MEG experiment at the Paul Scherrer Institut (PSI) represents the state of the art in the search for the charged Lepton Flavor Violating $\mu^+ \to e^+\gamma$ decay, setting the most stringent upper limit on the BR $(\mu^+ \to e^+\gamma) \leq 4.2 \times 10^{-13}$ (90% C.L.). An upgrade of MEG, MEG II, was designed, commissioned and recently started the physics data taking. Its goal is to reach a sensitivity level of 6×10^{-14}. In order to reconstruct the positron momentum vector a Cylindrical Drift CHamber (CDCH) with unprecedented peculiarities was built, featuring angular and momentum resolutions at the 6.5 mrad and 100 keV/c level. The CDCH is a 2-meter long, 60 cm in diameter, low-mass, single volume detector with high granularity: 9 layers of 192 drift cells, few mm wide, defined by ~12000 wires in a stereo configuration for longitudinal hit localization. The filling gas mixture is Helium:Isobutane 90:10. The total radiation length is 1.5×10^{-3} X_0, thus minimizing the Multiple Coulomb Scattering and allowing for a single-hit resolution < 120 μm. After the assembly at INFN Pisa, the CDCH was transported to PSI and integrated into the MEG II experimental apparatus since 2018. The commissioning phase lasted for the past three years until the operational stability was reached in 2020. The analysis software is continuously developing and the tuning of the reconstruction algorithms is one of the main activities. The latest updates on the positron momentum vector resolutions and tracking efficiency are presented.

1. The MEG II Cylindrical Drift CHamber (CDCH)

Design. The Cylindrical Drift CHamber (CDCH) [1] is a key detector to improve the reconstruction performances on the positron kinematic variables, increase the geometric acceptance and efficiency for 50 MeV e^+ and guarantee the proper operation at high rates with long-term detector stability. In order to reach the MEG II experimental requirements a low-mass, single volume detector with high granularity was built at the INFN Pisa (Italy) and is currently in the physics data taking phase at the Paul Scherrer Institut (PSI, Switzerland). Together with the pixelated Timing Counter (pTC) [2], whose scintillator tiles read out by SiPMs are used to measure the positron time at the 35 ps level, it is part of the MEG II e^+ spectrometer, which exploits the COBRA superconducting gradient-field magnet. The CDCH ensures the full azimuthal coverage around the μ^+ beam stopping target, featuring a cylindrical shape with a length of ~191 cm and a diameter of ~60 cm. The external radius is constrained by the available space inside the COBRA magnet, while its length is dictated by the necessity of tracking the particle trajectories up to the pTC. This reduces any passive material

* Corresponding author.
E-mail address: marco.chiappini@pi.infn.it (M. Chiappini).

https://doi.org/10.1016/j.nima.2022.167740
Received 14 July 2022; Received in revised form 1 November 2022; Accepted 3 November 2022
Available online 13 November 2022
0168-9002/

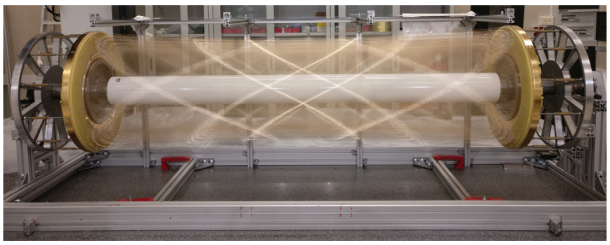

Fig. 1. The fully wired MEG II CDCH.

along the e^+ path, minimizing the contribution of the uncertainty in the track length measurement to the total timing resolution. This also increases the e^+ reconstruction efficiency, i.e. tracks reconstructed in the drift chamber with corresponding hits in the pTC, up to ∼70%, almost a factor of two better than the old MEG tracking system. The internal radius is large enough so that low energy e^+ are swept away by the gradient magnetic field without crossing the sensitive volume. On the other hand, e^+ with momentum larger than ∼45 MeV/c are tracked until they reach the pTC scintillation tiles. The CDCH active region extends radially for $\Delta R \sim 8$ cm and it is formed by 9 concentric layers of 192 drift cells each, defined by 11 904 wires. The high density of sensitive elements allows us to exploit four times more hits on average compared to the previous MEG tracker. A single drift cell is quasi-square with a 20 μm gold-plated tungsten sense wire surrounded by 40/50 μm silver-plated aluminum field wires, with a 5:1 field-to-sense wires ratio. The wires are not parallel to the CDCH axis, but form an angle varying from 6° in the innermost layer (L9) to 8.5° in the outermost layer (L1). This stereo angle has an alternating sign, depending on the layer, allowing the reconstruction of the longitudinal hit coordinate Z. The cell width varies from 5.8 mm to 7.5 mm at the CDCH center and from 6.7 mm to 8.7 mm at the endplates, keeping the occupancy at a sustainable level, especially for the inner layers placed at ∼17 cm from the beam axis (∼1.5 MHz/cell). The gas mixture is He:iC_4H_{10} (90:10) [3], a good compromise between transparency and single-hit resolution, measured on prototypes to be $\sigma_H < 120$ μm [4]. Some additives are used to reach the operational stability. All the aforementioned features guarantee an extremely low material budget, for the γ background (from bremsstrahlung and annihilation-in-flight) reduction and the minimization of the multiple Coulomb scattering. The total radiation length is $\sim 1.5 \times 10^{-3}$ X_0 per track turn.

Construction. Given the extremely high wire density (12 wires/cm^2) the CDCH features a modular construction [5]. The wires are not strung directly on the chamber but fixed at both ends on the pads of two PCBs (wire-PCBs), which are then radially stacked in the twelve 30°-sectors of the spoke-wheel-shaped aluminum endplates (Fig. 1). The wiring phase exploits a custom-made machine with a wire positioning accuracy of ∼20 μm and a semi-automatic laser soldering. PEEK spacers, whose thickness is tuned through geometry survey campaigns during the building phase, are used to have the correct radial dimensions of the drift cells. The azimuthal dimensions are defined by the pad spacing in the wire-PCBs. A 1.8 mm-thick Carbon Fiber (CF) support structure is connected to the outer endplate radius, featuring a structural and gas mixture tightness function. It keeps the endplates at the correct distance, ensuring the proper mechanical wire tension. A 20 μm one-side-aluminized Mylar foil is connected to the inner endplate radius, separating the CDCH gas volume from the He-filled target region, both kept a few Pascals above the atmospheric pressure with a continuous flow. Wiring, assembly and maintenance phases are performed inside cleanrooms. The assembly station allows to adjust and record the chamber geometry[1] thanks to a coordinate measuring machine and a laser tracker at the 20 μm level. The CDCH construction lasted from late 2016 to early 2018.

[1] Endplate planarity, parallelism and mutual distance.

2. CDCH commissioning

The detector commissioning [6] started in summer 2018 with the CDCH transport to PSI and it lasted 3 years with continuous improvements both in the hardware and software. The CDCH integration in the MEG II experimental apparatus was successfully tested in the 2018 engineering run and confirmed during the activities in 2019, 2020 and 2021, including the signal and HV cabling as well as the cooling and gas mixture distribution piping. Additional structures are connected to the endplates in $\pm Z$-directions: aluminum extension cylinders are installed at the inner radius to couple the chamber to the MEG II beam line; CF cylindrical covers are mounted at the outer radius to enclose the endcap regions. The CDCH mechanics proved to be stable (at ∼ few μm level) and adequate to sustain a full MEG II run. The full operational stability was reached in 2020.

Final working point. Inside the endcap regions 216 Front-End (FE) boards [7] per side are plugged to the wire-PCBs. The ionization signal is read out from the Up-Stream (US) and Down-Stream (DS) sides to improve the hit Z reconstruction with the charge division and time difference methods. Each board features eight differential channels, a low-noise double amplification stage and a high bandwidth (∼400 MHz). A dedicated cooling system based on a 1 kW chiller and a cold water distribution system with piping embedded in the board holders is used. Dry air is flushed inside the endcaps to avoid water condensation and dangerous temperature gradients. The environmental conditions are continuously monitored through several sensors. The High-Voltage (HV) is applied from the US side, with the Working Point (WP) chosen to have a gas gain[2] $G_G = 5 \times 10^5$. A HV tuning of 10 V/layer, ranging from 1400 V for L9 to 1480 V for L1, is used to compensate for the variable cell dimensions with R and Z due to the stereo geometry. The CDCH electrostatic stability was experimentally found through systematic HV tests at different endplate distances/CDCH lengthening to account for possible deviations from the nominal geometry due to the modular assembly. The final wire elongation is set to +5.2 mm (65% of the elastic limit).

Problems along the path. During the construction and commissioning of the detector two main problems were faced and finally solved. The first one is the breaking of 107 Al(Ag) cathode wires. In particular the 40 μm wires were affected (96 wires, 90%). This problem was deeply investigated [8] performing optical inspections with microscopes, chromatography, practical dip tests in water and SEM/EDX analyses. The origin of the breaking was found to be the galvanic corrosion of the Al core caused by the air moisture condensation inside cracks in the Ag coating, even at very low relative humidity levels < 30%. We found a good linear correlation between the number of broken wires and exposure time to humidity. The problem was then fully cured by keeping the CDCH volume in an inert atmosphere. We built a dedicated tool and developed a safe procedure to extract all the broken wire pieces from the chamber and avoid random shorts which would have made large parts of the detector not operational. Thanks to the cathode wire redundancy, electric field simulations confirmed a negligible impact of a missing cathode wire on isochrones and thus on e^+ reconstruction. The wire breaking phenomenon seems related also to the second problem, occurred during the detector operation in 2019, after an anode–cathode short circuit. This was caused by a very short wire segment not seen during a previous broken wire extraction procedure and thus remained inside the chamber. We observed an abrupt increase in current up to 400 μA during nominal operations. Investigations began immediately. The CDCH external CF shell was replaced by a transparent Plexiglas one and we were able to directly spot the origin of the high currents through dedicated HV tests with the standard gas mixture. Corona-like discharges were seen in correspondence of six whitish regions[3]

[2] To be sensitive to the single ionization cluster and exploit cluster timing techniques. Simulations on single electron gain are made with the Garfield software (https://garfieldpp.web.cern.ch/garfieldpp/).

[3] The size is of the order of 10–20 cm azimuthally, a few cm longitudinally and fully radially developed.

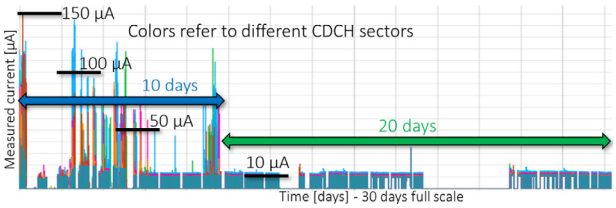

Fig. 2. Conditioning period with μ^+ beam and 2% O_2 content (blue arrow, 10 days). The higher current level (up to 150 μA) is visible before reaching the operational stability around 10 μA (green arrow).

on the wires. SEM/EDX analyses highlighted the presence of sulfur traces. Accelerated aging tests on prototypes [9] returned no design issues or discharges. We then started in 2020 a dedicated optimization of the standard gas mixture. Several additives were tried to recover the normal detector operation. The reduction of the high currents was achieved with an oxygen level up to 2%, then gradually lowered to avoid attachment effects. In addition, isopropyl alcohol proved to be crucial to keep the current level stable. The CDCH is now operated at the HV WP in stable conditions at full MEG II beam intensity with the standard gas mixture + isopropyl alcohol (1.5%) + O_2 (0.5%)[4].

Conditioning. The detector conditioning is a crucial operation to ensure a stable data taking period. The initially high currents (up to $I \sim 150$ μA, Fig. 2) resulting from the e^+ ionization at increasing μ^+ beam intensity (R_μ) are lowered by raising the O_2 content in the gas mixture up to 2%. Once recovered the I vs. R_μ proportionality, the O_2 content is gradually reduced to 0.5%, while the isopropyl alcohol is kept constant at 1.5%. The measured stable current (10–20 μA range) translated in accumulated charge/cm is in agreement with the design value: ~0.1 C/year/cm. The gain curves show the expected variations with the atmospheric pressure P, according to $\Delta G_G/G_G = -k(\Delta P/P)$, where k is a constant.

3. Preliminary performances

The CDCH performances were evaluated since the engineering runs 2018, 2019 and 2020. During the 2021 physics run the full electronics read out was available for the first time. The chamber operational stability and data acquisition chain, including a complete noise and signal check of all the DAQ channels, were positively tested. A great analysis effort is currently ongoing to tune the reconstruction algorithms with continuous developments and improvements. In MEG II the full signal waveform is recorded, then a fine analysis is made offline to get the hit information (timing, signal amplitude and integral, position in the detector). The signal amplitude distributions show a good uniformity between different layers, a confirmation that the 10 V scaling of the HV works.

HV scans around the WP with different ionization sources (e^+ from μ^+ decays and cosmic rays) allowed to obtain the measurement of the gas gain $G_G = (2\text{–}4) \times 10^5$, in agreement with the expectation (Fig. 3). The full detector occupancy was successfully tested (Fig. 4). With the detector equipped with the full DAQ electronics the hit detection efficiency, the pattern recognition algorithm and the tracking performance were evaluated on data to get the first experimental resolutions on the e^+ track parameters and efficiency. Fig. 5 shows an example of a fitted e^+ track.

The current full MC tracking performances are quoted: momentum resolution $\sigma_p = 87$ keV/c; angular resolutions $\sigma_\theta = 6.8$ mrad, $\sigma_\phi = 5.4$ mrad; position resolutions at target $\sigma_Z = 1.8$ mm, $\sigma_Y = 0.8$ mm;

[4] From 2020 measurements we do not observe a significant gain reduction, only a limited efficiency decrease when O_2 was at 1%, then reduced to the current value.

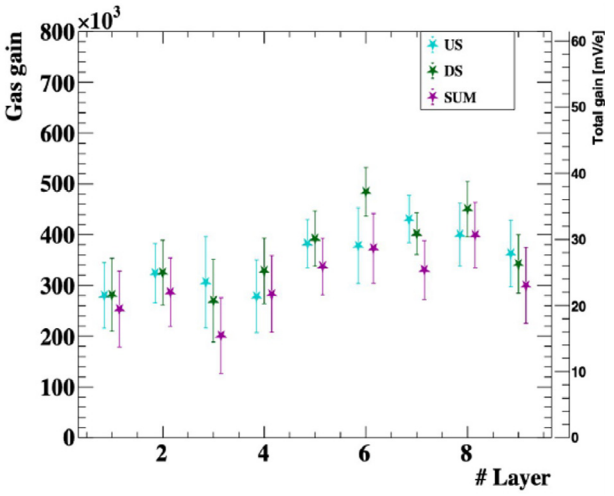

Fig. 3. Gas gain vs. layer number. G_G is computed using the signal amplitude recorded from one wire end or the sum of the two sides (different colors).

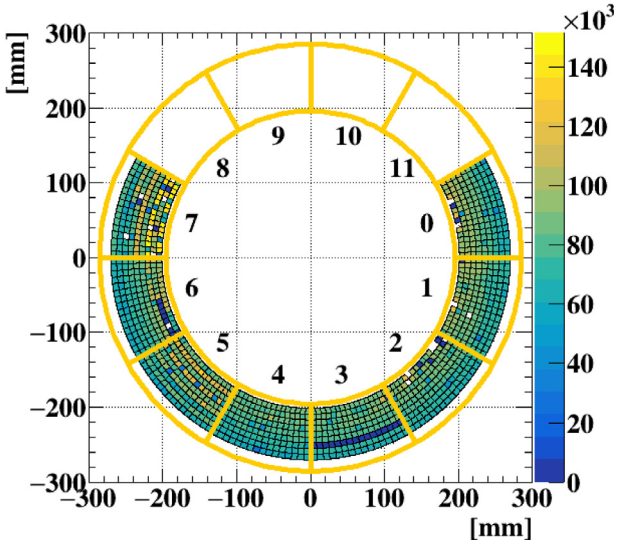

Fig. 4. Example of CDCH occupancy (number of hits per drift cell) with 2021 full readout. The four upper sectors are out of acceptance for signal e^+ and are usually not read out. The dead channels (blue cells) were recovered during the 2022 maintenance work.

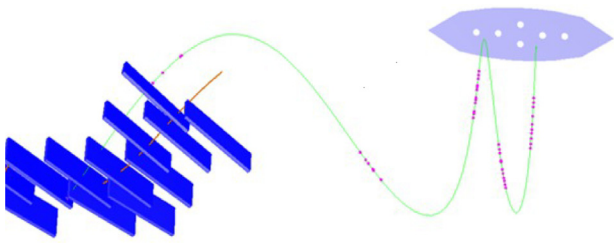

Fig. 5. Example of fitted e^+ track (green) starting from the μ^+ stopping target (violet) with the corresponding CDCH hits (magenta) and pTC tiles (blue).

positron efficiency (CDCH tracking × pTC matching) $\epsilon = 70\%$. With the last software version, the analysis of 2021 data returns: $\sigma_p \sim$

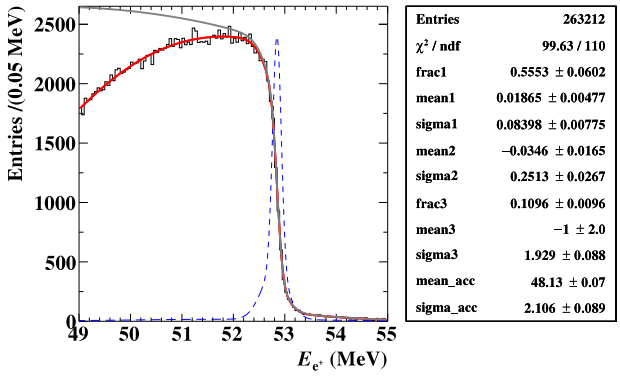

Fig. 6. Reconstructed e^+ energy from μ^+ decay fitted (solid red line) with [theoretical spectrum (solid black line) × acceptance] ⊗ triple-Gaussian resolution function (dashed blue line).

84 keV/c (Fig. 6); σ_θ = 7.8 mrad, σ_ϕ = 6.2 mrad; σ_Z = 2.4 mm, σ_Y = 0.9 mm; $\epsilon \sim 65\%$. Big improvements are under development to reach the MC values. The hit-track residual σ_{HT} gives a measurement of how misalignments, σ_H and other systematics (B field) combine to determine the reconstruction performance. After the application of the hardware (from geometry survey measurements) and software (preliminary) detector alignment σ_{HT} is 140 μm, a good starting result. A further big improvement is expected to be achieved soon by exploiting a refined track-based alignment of the drift cells.

4. Conclusions

Despite the COVID-19 pandemic we completed the commissioning of all the MEG II sub-detectors in 2021 and the experiment recently started the physics data taking. The CDCH faced two major problems along the path: corrosion of Al wires and high currents. Both were solved with great efforts. The preliminary results from 2020–2021 data analysis have been presented.

Acknowledgments

This work was partially supported by JSPS KAKENHI JP21H04991, JP21H00065 and JPJSCCA20180004.

References

[1] M. Chiappini, et al., The new drift chamber of the MEG II experiment, Nucl. Instrum. Methods A 936 (2019) 501–502, http://dx.doi.org/10.1016/j.nima.2018.10.182.

[2] M. Nishimura, et al., Full system of positron timing counter in MEG II having time resolution below 40 ps with fast plastic scintillator readout by SiPMs, Nucl. Instrum. Methods A 958 (2020) 162785, http://dx.doi.org/10.1016/j.nima.2019.162785.

[3] A.M. Baldini, et al., Gas Distribution and Monitoring for the Drift Chamber of the MEG II Experiment, J. Instrum. 13 (06) (2018) P06018, http://dx.doi.org/10.1088/1748-0221/13/06/P06018.

[4] A.M. Baldini, et al., Single-hit resolution measurement with MEG II drift chamber prototypes, J. Instrum. 11 (2016) P07011, http://dx.doi.org/10.1088/1748-0221/11/07/P07011.

[5] G. Chiarello, et al., The construction technique of the high granularity and high transparency drift chamber of MEG II, J. Instrum. 12 (07) (2017) C07022, http://dx.doi.org/10.1088/1748-0221/12/07/c07022.

[6] M. Chiappini, et al., Commissioning of the MEG II tracker system, J. Instrum. 15 (06) (2020) C06056, http://dx.doi.org/10.1088/1748-0221/15/06/c06056.

[7] G. Chiarello, et al., A high performance Front End Electronics for drift chamber readout in MEG experiment upgrade, Nucl. Instrum. Methods A 824 (2016) 336–339, http://dx.doi.org/10.1016/j.nima.2015.11.092.

[8] A. Baldini, et al., Detailed analysis of chemical corrosion of ultra-thin wires used in drift chamber detectors, J. Instrum. 16 (12) (2021) T12003, http://dx.doi.org/10.1088/1748-0221/16/12/t12003.

[9] M. Venturini, et al., Ageing tests for the MEG II drift chamber, Nucl. Instrum. Methods A 824 (2016) 592–594, http://dx.doi.org/10.1016/j.nima.2015.09.030.